Combustion and Flame 156 (2009) 250–260

Contents lists available at ScienceDirect

Combustion and Flame

www.elsevier.com/locate/combustflame

# A jet-stirred reactor and kinetic modeling study of ethyl propanoate oxidation

W.K. Metcalfe [a,*], C. Togbé [b], P. Dagaut [b], H.J. Curran [a], J.M. Simmie [a]

[a] Combustion Chemistry Centre, National University of Ireland, Galway, Ireland
[b] CNRS I.C.A.R.E., 1C, Avenue de la Recherche Scientifique, 45071 Orléans Cedex 2, France

ARTICLE INFO

*Article history:*
Received 22 February 2008
Received in revised form 3 June 2008
Accepted 15 September 2008
Available online 20 October 2008

*Keywords:*
JSR
Oxidation
Ethyl propanoate
Modeling

ABSTRACT

A jet-stirred reactor study of ethyl propanoate, a model biodiesel molecule, has been carried out at 10 atm pressure, using 0.1% fuel at equivalence ratios of 0.3, 0.6, 1.0 and 2.0 and at temperatures in the range 750–1100 K with a constant residence time of 0.7 seconds. Concentration profiles of ethyl propanoate were measured together with those of major intermediates, ethylene, propanoic acid, methane and formaldehyde, and major products, water, carbon dioxide and carbon monoxide. This data was used to further validate a previously published detailed chemical kinetic mechanism, containing 139 species and 790 reversible reactions. It was found that this mechanism required a significant increase in the rate constant of the six-centered unimolecular elimination reaction which produces ethylene and propanoic acid in order to correctly reproduce the measured concentrations of propanoic acid. The revised mechanism was then used to re-simulate shock tube ignition delay data with good agreement observed. Rate of production and sensitivity analyses were carried out under the experimental conditions, highlighting the importance that ethylene chemistry has on the overall reactivity of the system.



## 1. Introduction

The contribution that the transport sector makes to the high level of carbon dioxide present in the atmosphere has been highlighted in a report from the Intergovernmental Panel on Climate Change [1]. This report recommended the global use of biofuels to help reduce $CO_2$ emissions. An increasingly popular biofuel is biodiesel, composed of a mixture of saturated and unsaturated long-chain methyl and ethyl esters. Direct studies of typical biodiesels are difficult both because laboratory experiments must be carried out on complex, largely involatile, mixtures and also because the modeling and simulation is not sufficiently developed to be able to tackle such large molecules [2]. For this reason, short chain molecules containing the same functional group as real biodiesel are studied to gather insights into the oxidation behaviour of the practical fuel.

Dagaut et al. [3] studied the oxidation of an actual biodiesel in the form of rape seed oil methyl ester (RME). The study was performed in a jet-stirred reactor between 1 and 10 atm and over the temperature range 800–1400 K, for residence times of 0.07 and 0.1 s at 1 atm, and 1.0 s at 10 atm. Experiments were performed at four equivalence ratios: $\phi = 0.25$, 0.5, 1.0, and 1.5, with an initial fuel concentration of 0.05%. RME is a complex mixture of $C_{14}$, $C_{16}$, $C_{18}$, $C_{20}$, and $C_{22}$ esters. Due to this complexity, the authors proposed the use of a detailed chemical kinetic mechanism for *n*-hexadecane to simulate the reactivity of RME. They found that the *n*-hexadecane model produced a good description of the overall reactivity of RME and reproduced the experimental results in terms of the relative importance of the olefins ($C_2$–$C_6$) produced.

Methyl butanoate (MB), with a structural formula of $CH_3CH_2$-$CH_2C(O)OCH_3$, has proven to be the most popular choice as a biodiesel surrogate, with several studies published in recent years. In 2000, Fisher et al. [4] published a detailed chemical kinetic mechanism of MB oxidation but only had relatively unsophisticated experiments to validate their work [5–8].

In 2004, Marchese et al. [9] studied MB oxidation in a flow reactor at 12.5 atm. Concentrations of 800 ppm were examined over equivalence ratios of 0.35, 1.0 and 1.5. Reactant, intermediate and product species were quantified at a residence time of 1.8 s over the temperature range 500–900 K. The Fisher mechanism was used to simulate these results and was found to be in good agreement under stoichiometric conditions, but over-predicted reactivity at fuel rich conditions whilst under-predicting reactivity at lean conditions.

This data was reported by Gaïl et al. [10] together with data from a jet-stirred reactor (JSR) and an opposed-flow diffusion flame. MB and a host of intermediate species were quantified at a residence time of 70 ms in the JSR at an equivalence ratio of 1.13 over the temperature range 800–1275 K at 1 atm using 0.075% MB diluted in nitrogen. The opposed-flow diffusion flame measurements were performed for a stream of 4.7% MB diluted in $N_2$ at the bottom inlet and a stream of 42% $O_2$ also diluted in $N_2$ at the top inlet. MB and a host of intermediate species were

* Corresponding author.
*E-mail address:* wayne.metcalfe@nuigalway.ie (W.K. Metcalfe).

0010-2180/$ – see front matter 
doi:10.1016/j.combustflame.2008.09.007

again quantified. Simulations using a slightly modified version of the Fisher model reproduced the flow reactor data at $\phi = 0.35$ and $\phi = 1.0$; however, reactivity at $\phi = 1.5$ was greatly overpredicted. Agreement with JSR data was reasonable, although activity was underpredicted at low temperatures for MB and various intermediate species. The same model was not able to reproduce the opposed-flow diffusion flame data, showing, in general, higher reactivity for intermediate species and lower reactivity for MB than observed in experiment.

This opposed-flow diffusion data was also presented by Sarathy et al. [11] coupled with additional JSR data in a comparative experimental study of the oxidation of MB and an unsaturated methyl ester, methyl crotonate ($C_5H_8O_2$). The peak major intermediate species mole fractions were reported coupled with other select species, including MB. The experiments were carried out at a residence time of 70 ms, over the temperature range 850–1350 K for a mixture of 0.075% MB under stoichiometric conditions at 1 atm pressure.

Schwartz et al. [12] studied the effect of doping a methane/air nonpremixed flame with 5000 ppm of MB, measuring major species from within the flame using mass spectrometry. The study showed that the rate of MB decomposition was explained by a unimolecular decomposition reaction:

$$\mathrm{MB} \longleftrightarrow \mathrm{C_3H_7C(O)\dot{O}} + \dot{\mathrm{C}}\mathrm{H_3}.$$

A recent study of MB was carried out by the Combustion Chemistry Centre ($C^3$) at the National University of Ireland, Galway and reported by Dooley et al. [13]. MB oxidation was examined behind reflected shock waves at pressures of 1 and 4 atm over the temperature range 1250–1760 K. The shock tube study was complemented by a rapid compression machine study over the temperature range 640–949 K at compressed gas pressures of 10, 20 and 40 atm at equivalence ratios of 0.33, 0.5 and 1.0. This data coupled with speciation data reported in the literature from a flow reactor [9,10], a jet-stirred reactor [10,11], and an opposed-flow diffusion flame [10], was used to produce a detailed chemical kinetic model of MB oxidation. The model successfully reproduced the effect of equivalence ratio, fuel concentration and pressure for the shock tube ignition delay times. The agreement with rapid compression machine ignition delays was less accurate, although the qualitative agreement was reasonable. The model reproduced most speciation data with good accuracy. Sensitivity and flux analysis was also carried out, highlighting the importance of unimolecular fuel decomposition at high temperatures, reactions involving the $\mathrm{H\dot{O}_2}$ radical at low to intermediate temperatures, and the importance of fuel alkyl radical decomposition under fuel-rich conditions.

The focus of the current study is to understand the oxidation of ethyl propanoate (EP), a short chain ethyl–ester, which is also an appropriate choice as a model biodiesel molecule. It shares the same molecular formula as MB, but has a different structure, $CH_3CH_2C(O)OCH_2CH_3$. There are few previous studies of ethyl propanoate (or propionate). Blades and Gilderson [14] studied the kinetics of the thermal decomposition of ethyl propanoate in a toluene gas carrier system, measuring the rate constant of the six-centered elimination reaction producing propanoic acid and ethylene. A rate expression of $5.2 \times 10^{12} \exp(-48{,}500 \pm 350/RT)$ $\mathrm{s^{-1}}$ ($E_a$ in cal $\mathrm{mol^{-1}}$) was determined over the temperature range 780–875 K by titration of the propanoic acid.

The activation energy recommended by Blades and Gilderson of 48.5 kcal $\mathrm{mol^{-1}}$ is in very good agreement with the later work of O'Neal and Benson [15] who calculated an activation energy of 48.1 kcal $\mathrm{mol^{-1}}$ using transition state theory.

In addition, Blades and Sandhu [16] studied the pyrolysis of ethyl formate to formic acid and ethylene over the temperature range 830–903 K. This reaction proceeds through a similar six-centered transition state as the ethyl propanoate decomposition with an activation energy of $48.1 \pm 0.5$ kcal $\mathrm{mol^{-1}}$.

The thermal decomposition of ethyl propanoate was also measured behind reflected shock waves by Barnard et al. [17], with their results reproducing the results of Blades and Gilderson with an activation energy of 48.5 kcal $\mathrm{mol^{-1}}$.

The more recent calculations of El Nahas et al. [18] produced an activation energy of 50.0 kcal $\mathrm{mol^{-1}}$ which is also in good agreement with previous experiments and calculations.

Schwartz et al. [12] have studied the effect of doping a methane/air nonpremixed flame with 5000 ppm of ethyl propanoate (EP). They found that a unimolecular six-centered dissociation reaction explains their results:

$$\mathrm{EP} \longleftrightarrow \mathrm{C_2H_5COOH} + \mathrm{C_2H_4}. \qquad \text{(R672)}$$

A shock tube ignition delay study of ethyl propanoate was previously carried out at $C^3$ and reported in Metcalfe et al. [19]. Ethyl propanoate oxidation was examined behind reflected shock waves at 1 and 4 atm, over the temperature range 1100–1670 K and for equivalence ratios of 0.25, 0.5, 1.0 and 1.5. A chemical kinetic mechanism was developed and validated against the shock tube ignition delay times with good agreement observed between simulation and experiment. Through sensitivity and flux analysis, the importance of the six-centered elimination reaction producing propanoic acid and ethylene was highlighted. This study also compared the reactivity of ethyl propanoate to methyl butanoate, with the former found to be more reactive over the conditions studied. The higher reactivity of ethyl propanoate was due to the reactivity of the two major intermediates, namely ethylene and propanoic acid.

## 2. Experimental

A spherical fused jet-stirred reactor (JSR) [20] was used to carry out the experimental study. It was located inside a regulated electrical resistance system of approximately 1.5 kW, surrounded by insulating material and a pressure-resistant jacket, allowing operation up to 10 atm. Ethyl propanoate (B.P. 99 °C/M.P. −73 °C) was provided by Sigma-Aldrich at > 99% purity. Ethyl propanoate was pumped using a micro-piston HPLC pump and sent to an atomizer-vaporizer assembly maintained at 130 °C. A flow of nitrogen (100 L $\mathrm{h^{-1}}$) was used for the atomization. The oxygen (99.995% pure) and nitrogen flow-rates were measured and regulated by thermal mass flow controllers (Brooks 5850E). Ethyl propanoate and oxygen were diluted by a flow of nitrogen and mixed at the entrance of the injectors after pre-heating. The exact composition of mixtures used in this study are provided in Table 1.

Residence time distribution studies showed that the reactor operates under macro-mixing conditions. As previously shown [21–25], a good thermal homogeneity was recorded along the vertical axis of the reactor by thermocouple measurements (Pt/Pt–Rh 10%, 0.1 mm diameter inside a thin-wall fused-silica tube to prevent catalytic reactions on the wires). Typical temperature gradients of < 2 K $\mathrm{cm^{-1}}$ were measured. Since the experiments were carried out under a high degree of dilution (EP concentration = 1000 ppmv), the temperature rise due to the reaction was generally < 30 K.

**Table 1**
Percentage composition of EP/$O_2$/$N_2$ mixtures studied in the JSR.

| $\phi$ | EP | $O_2$ | $N_2$ |
|---|---|---|---|
| 0.30 | 0.1 | 2.166 | 97.733 |
| 0.60 | 0.1 | 1.080 | 98.820 |
| 1.00 | 0.1 | 0.650 | 99.250 |
| 2.00 | 0.1 | 0.325 | 99.575 |

Samples of the reacting mixtures were taken by sonic probe sampling and collected in 1 L Pyrex bulbs at approximately 40 Torr for immediate gas chromatography (GC) analyses as in [23–25]. Capillary columns (Poraplot U $Al_2O_3$/KCl, DB-624, and Carboplot P7) were used with a thermal conductivity detector (TCD) and a flame ionization detector (FID) for the measurements of gases. Helium was used as a carrier gas. Online Fourier transform infrared (FTIR) analyses of the reacting gases were also performed by connecting the sampling probe to a temperature controlled (140 °C) gas cell (10 m path length) via a Teflon heated line (160 °C). The sample pressure in the cell was 200 mbar.

This analytical equipment allowed the measurements of ethyl propanoate, propanoic acid, propene, ethane, ethylene, acetylene, formaldehyde, methane, carbon dioxide, carbon monoxide, water and hydrogen. As previously reported [21–25], very good agreement between the GC and FTIR measurements was found for the compounds measured by both techniques (CO and $CO_2$). The carbon balance was checked for every sample and found to be good ($100 \pm 5\%$).

## 3. Kinetic modeling

All of the modeling computations in this study were carried out using the HCT modeling code [26]. Simulations were performed under isothermal, constant pressure conditions, and assumed perfect mixing of the reactants. Time dependent calculations were run for long times until a steady-state solution was obtained. The thermodynamic properties for the relevant radicals and stable parents were obtained using Benson's [27] group additivity method employing THERM [28] with updated H/C/O groups and bond dissociation groups [29].

The detailed chemical kinetic model used in this study is based on a mechanism previously developed at C$^3$ to simulate shock tube ignition delay times for ethyl propanoate. A complete listing and description of ethyl propanoate oxidation can be found in Metcalfe et al. [19], while the main features of the mechanism are summarized here.

The ethyl propanoate sub-mechanism was created by analogy to methyl butanoate [4]. A six-centered elimination reaction was added to describe the decomposition of ethyl propanoate to propanoic acid and ethylene. The frequency factor for this reaction was taken from O'Neal and Benson [15] and the activation energy from El-Nahas et al. [18].

The ethylene sub-mechanism was based on previous work by Curran et al. for dimethyl ether oxidation [30–33]. This sub-mechanism was validated against speciation data in two distinct jet-stirred reactors [34,35] and also against shock tube ignition delay times [36]. The model was in good agreement with species profiles showing that the chemistry producing intermediate species is reliable. The simulation was in reasonable agreement with the ignition delay times, with the model too slow over most conditions.

The propanoic acid sub-mechanism was developed in the study of Metcalfe et al. and was based on the work of Curran et al. [37,38] for *n*-heptane and iso-octane kinetic mechanism development. The rate constants used for primary hydrogen atom abstraction are those for primary hydrogen abstraction from an alkane. Rate constants for hydrogen atom abstraction of the "secondary" hydrogen atoms (i.e. $RCH_2(C{=}O)OH$) are taken to be identical to the similar hydrogen atom in methyl butanoate from the study of Fisher et al. [4]. The rate constants for the decomposition reactions of propanoic acid to methyl radical and $\dot{C}H_2COOH$, and methyl ketene and water were taken from Doolan et al. [39]. The sub-mechanism was tested against shock tube pyrolysis data of Doolan and correctly predicted propanoic acid consumption as a function of time.

Several changes have been made to the original ethyl propanoate mechanism in this current study in order to obtain better agreement with the jet-stirred reactor species profiles:

- The rate constant for the unimolecular elimination reaction producing ethylene and propanoic acid from ethyl propanoate,

$$EP \longleftrightarrow C_2H_4 + C_2H_5COOH, \tag{R672}$$

  was increased by a factor of four from $4.0 \times 10^{12} \exp(-50{,}000/RT)$ to $1.6 \times 10^{13} \exp(-50{,}000/RT)$ $s^{-1}$ ($E_a$ in cal mol$^{-1}$).
- The following abstraction reactions were decreased by a factor of two (Fig. 1):

$$EP + H\dot{O}_2 \longleftrightarrow EP2J + H_2O_2, \tag{R699}$$

$$EP + H\dot{O}_2 \longleftrightarrow EPEJ + H_2O_2, \tag{R700}$$

$$C_2H_5COOH + H\dot{O}_2 \longleftrightarrow CH_3\dot{C}HCOOH + H_2O_2. \tag{R770}$$

- An updated $C_3$ sub-mechanism was developed within the group and this has been incorporated into this version of the ethyl propanoate mechanism.

As mentioned above, the rate constant in the original paper [19] was derived from an *ab initio* calculation of the activation energy, with the frequency factor taken from the calculations of O'Neal and Benson. This rate constant is approximately 60% slower than that of Blades and Gilderson ($5.2 \times 10^{12} \exp(-48{,}500 \pm 350/RT)$ $s^{-1}$) at 850 K, primarily due to the 1.5 kcal difference in activation energy. Increasing the frequency factor by a factor of four has the effect of making the overall rate constant approximately 30% faster than that of Blades and Gilderson at 850 K. The frequency factor was altered instead of the activation energy, as the low temperature shock tube ignition delay times show significant sensitivity to the activation energy of this reaction.

It was found that decreasing the rate of the hydrogen abstraction reactions by $H\dot{O}_2$ at locations alpha to the (C=O)O in ethyl propanoate had the effect of reducing the concentration of $\dot{O}H$ ($H_2O_2 \longleftrightarrow \dot{O}H + \dot{O}H$), which slows down the consumption of propanoic acid. We feel this reduction is justified in that the electronegative $H\dot{O}_2$ may be repelled by the electronegative (C=O)O group, thus hindering the incoming $H\dot{O}_2$ radical and reducing the rate of reaction. The abstraction reaction of the similar hydrogen in propanoic acid was also decreased. These changes account for approximately 5% of the increase in propanoic acid concentration seen in Figs. 2–5.

Kinetic mechanisms are continually being developed and improved as more reliable descriptions of reactions become available. The new $C_3$ mechanism is based on that published in previous work on methane/propane mixtures [40], but some changes have been made, with the major ones described here. The rate constants cited in the text are provided in Table 2.

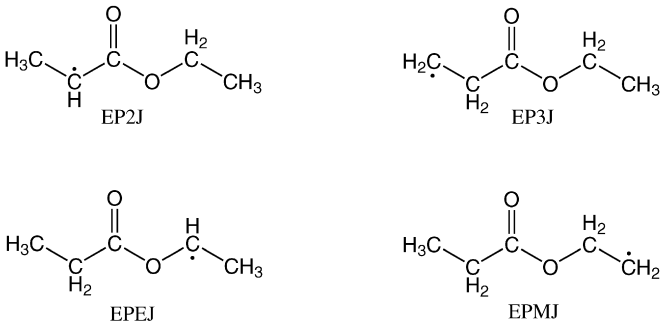


**Fig. 1.** Nomenclature of fuel-radical species.

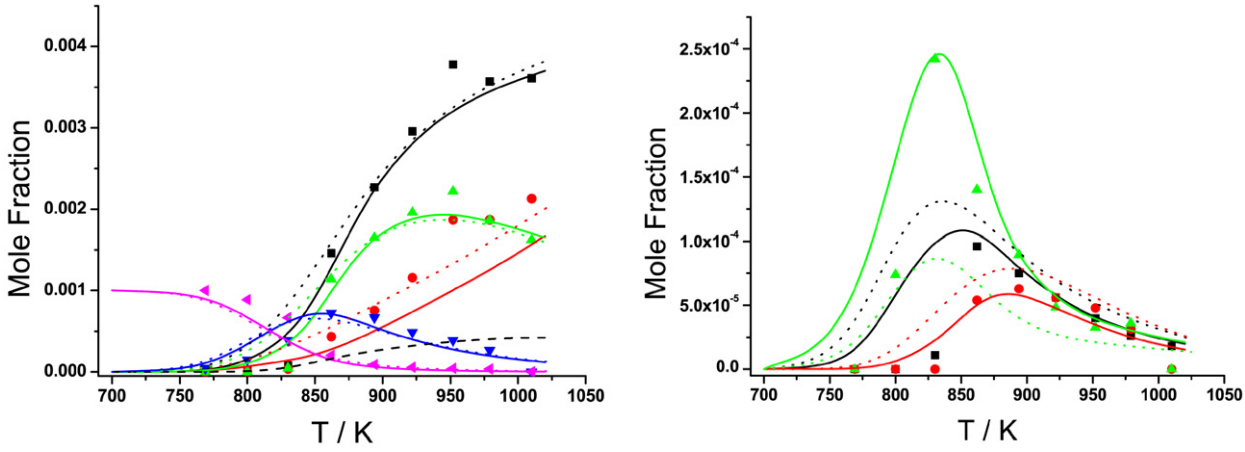


**Fig. 2.** Oxidation in the high pressure jet-stirred reactor of a 0.1% mixture of EP in $N_2$, $\phi = 0.3$, at 10 atm and 0.7 s residence time. (a) (◀) EP, (■) $H_2O$, (▲) CO, (●) $CO_2$, (▼) $C_2H_4$, (- - -) $C_2H_3COOH$ (prediction only). (b) (▲) $C_2H_5COOH$, (■) $CH_2O$, (●) $CH_4$. Symbols are experimental results. Dotted lines—Metcalfe et al. [19], solid lines—this study. (For interpretation of the references to colour in this figure legend, the reader is referred to the web version of this article.)

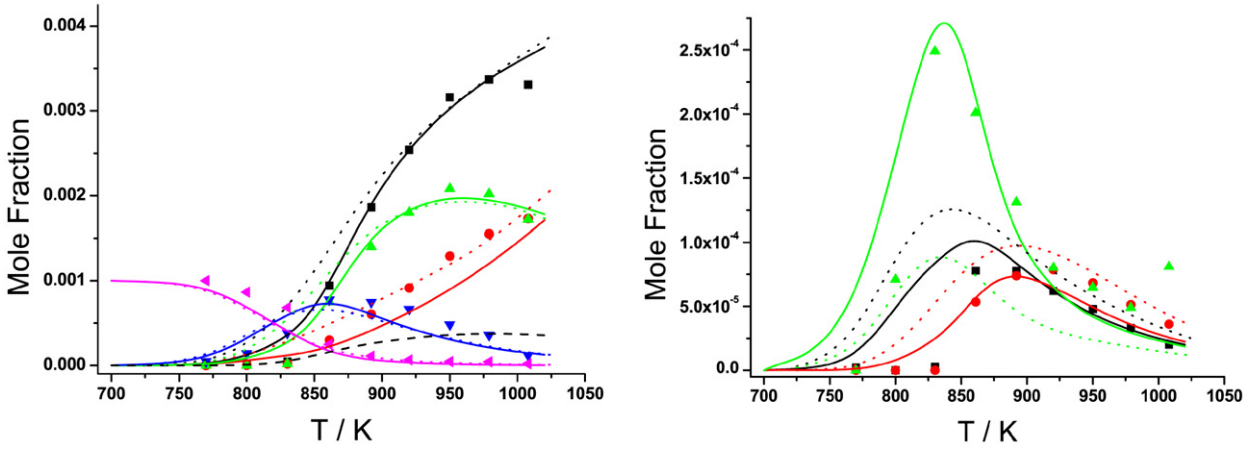


**Fig. 3.** Oxidation in the high pressure jet-stirred reactor of a 0.1% mixture of EP in $N_2$, $\phi = 0.6$, at 10 atm and 0.7 s residence time. (a) (◀) EP, (■) $H_2O$, (▲) CO, (●) $CO_2$, (▼) $C_2H_4$, (- - -) $C_2H_3COOH$ (prediction only). (b) (▲) $C_2H_5COOH$, (■) $CH_2O$, (●) $CH_4$. Symbols are experimental results. Dotted lines—Metcalfe et al. [19], solid lines—this study.

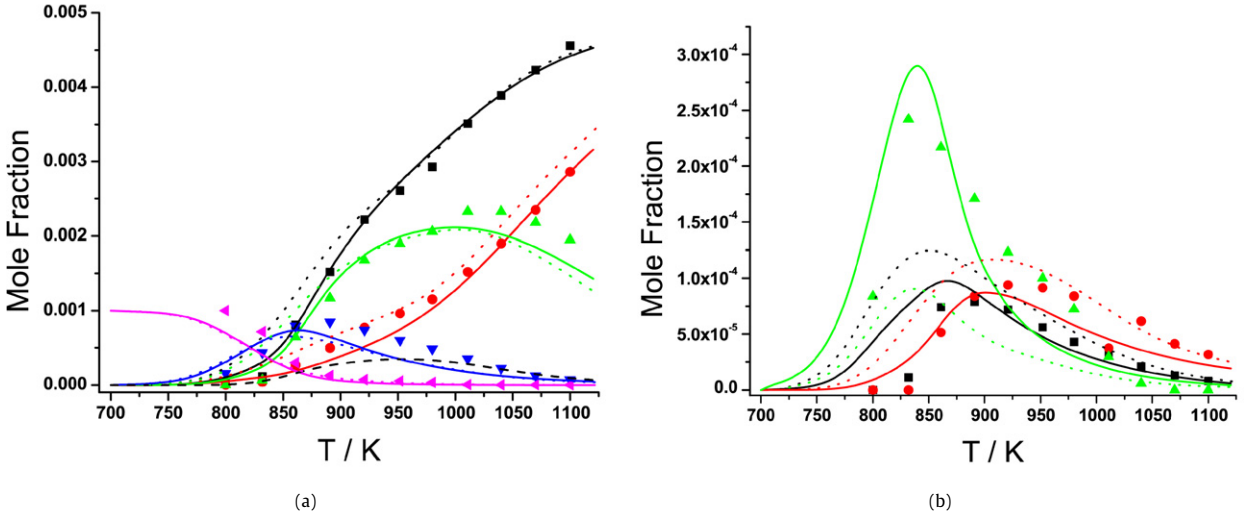


**Fig. 4.** Oxidation in the high pressure jet-stirred reactor of a 0.1% mixture of EP in $N_2$, $\phi = 1.0$, at 10 atm and 0.7 s residence time. (a) (◀) EP, (■) $H_2O$, (▲) CO, (●) $CO_2$, (▼) $C_2H_4$, (- - -) $C_2H_3COOH$ (prediction only). (b) (▲) $C_2H_5COOH$, (■) $CH_2O$, (●) $CH_4$. Symbols are experimental results. Dotted lines—Metcalfe et al. [19], solid lines—this study.

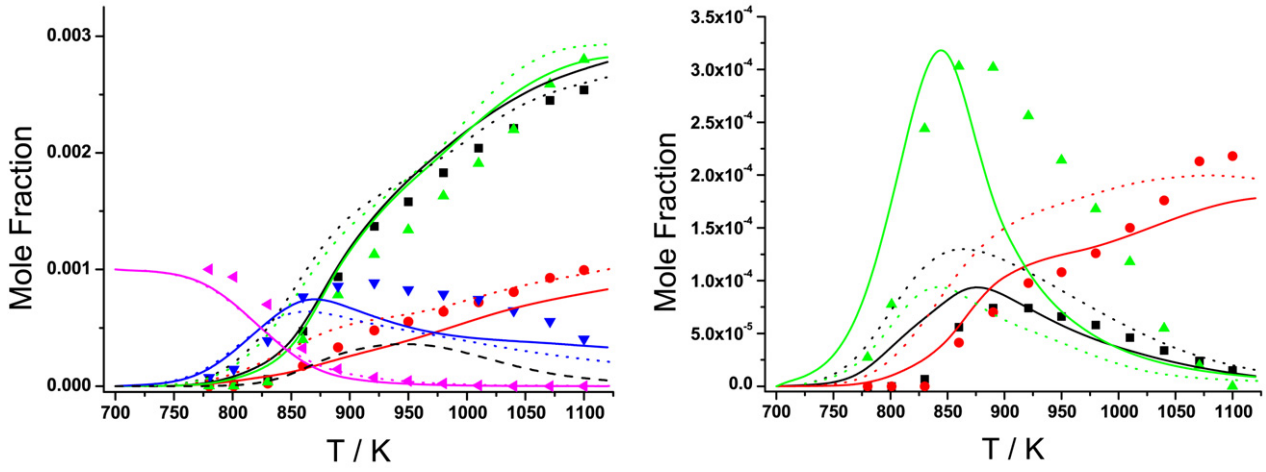


**Fig. 5.** Oxidation in the high pressure jet-stirred reactor of a 0.1% mixture of EP in $N_2$, $\phi = 2.0$, at 10 atm and 0.7 s residence time. (a) (◀) EP, (■) $H_2O$, (▲) CO, (●) $CO_2$, (▼) $C_2H_4$, (- - -) $C_2H_3COOH$ (prediction only). (b) (▲) $C_2H_5COOH$, (■) $CH_2O$, (●) $CH_4$. Symbols are experimental results. Dotted lines—Metcalfe et al. [19], solid lines—this study.

De Sain et al. [41] carried out a detailed analysis of the $\dot{C}_2H_5 + O_2$ system and we have adopted their rate constant recommendations at 10 atm. We have adopted the rate constant of Hessler [42] for

$$\dot{H} + O_2 \longleftrightarrow \dot{O} + \dot{O}H. \quad \text{(R1)}$$

You et al. [43] have recently reported on the rate constant for

$$CO + H\dot{O}_2 \longleftrightarrow CO_2 + \dot{O}H \quad \text{(R25)}$$

and we have adopted their value.

Recently, Srinivasan et al. [44] studied the reaction

$$CH_4 + O_2 \longleftrightarrow \dot{C}H_3 + H\dot{O}_2, \quad \text{(R110)}$$

and using both experimental results and calculations provided a rate constant in the temperature range 1655–1822 K. Jasper et al. [45] have calculated a rate constant expression for

$$\dot{C}H_3 + H\dot{O}_2 \longleftrightarrow \dot{C}H_3O + \dot{O}H \quad \text{(R109)}$$

which we have also adopted. The rate constant expression for

$$C_2H_6 + \dot{H} \longleftrightarrow \dot{C}_2H_5 + H_2 \quad \text{(R151)}$$

was taken from GRI-Mech 3.0 [46]. We have adopted the rate constant expression recommended in GRI-Mech 3.0 [46] for the reaction,

$$\dot{C}_2H_5 + M \longleftrightarrow C_2H_4 + \dot{H} + M, \quad \text{(R161)}$$

which is approximately a factor of two slower than the rate constant in our previous paper [40].

The new $C_3$ mechanism was validated against the same ethylene data [34–36] examined in the previous study [19] and it performed similarly, with at most a 10% discrepancy between predicted species profiles when compared to the ethyl propanoate mechanism reported in Metcalfe et al. The new $C_3$ mechanism had a greater effect on the shock tube ignition delay times simulated, with an average 25% difference between those previously reported, but achieves better agreement than the original mechanism with the data of Brown et al. [36].

Figures showing the mechanism's performance against both the propanoic acid and ethylene data can be found in the Supplementary material, together with the ethyl propanoate species thermochemistry and a complete explanation of the ethyl propanoate species naming scheme. The mechanism used in this study is available in Chemkin format at the Combustion Chemistry Centre's website [47].

## 4. Results and discussion

### 4.1. Experimental

Ethyl propanoate oxidation was studied in a high pressure jet-stirred reactor in which fuel, intermediate and product species profiles were recorded as a function of temperature. All of the experiments were carried out at a constant pressure of 10 atm, with a residence time of 0.7 s and with an ethyl propanoate concentration of 0.1%. Different equivalence ratios were examined by varying the oxygen concentration. The data collected is represented by the symbols in Figs. 2–5.

Ethyl propanoate ignites at approximately the same temperature over the four conditions studied, between 750–800 K. The main product concentrations change as the fuel/oxidizer mix moves from lean (Figs. 2 and 3), to stoichiometric (Fig. 4) and finally to rich, as shown in Fig. 5. Water is the major product at $\phi = 0.3$, 0.6 and 1.0 but is overtaken by carbon monoxide at the rich condition of $\phi = 2.0$. There is almost a factor of seven change in the oxygen concentration from $\phi = 0.3$ to $\phi = 2.0$, and the high concentration of carbon monoxide at the rich condition is coupled with the lowest concentration of carbon dioxide. Carbon monoxide is a product of incomplete combustion, so the decrease in its oxidation to $CO_2$ is to be expected with the decrease in oxygen concentration.

The main intermediate species observed are ethylene, propanoic acid, formaldehyde and methane. Ethylene and propanoic acid are the most abundant and are produced from the six-centered elimination reaction from the fuel.

### 4.2. Simulation

The performance of the original model [19] and the updated version from this study are also shown in Figs. 2–5.

Overall, the changes described in Section 3 have improved the performance of the model. The most significant change occurs in the prediction of the propanoic acid concentration profile. For example, in Fig. 2b, the updated model (solid green line) predicts the correct magnitude and the rate of consumption of the propanoic acid much more accurately than the previous mechanism (dotted green line).

Discrepancies exist between the mechanism's predictions and the experimental data under all conditions studied. The model over-predicts ethyl propanoate reactivity at all equivalence ratios,

**Table 2**
Ethyl propanoate mechanism rate coefficients; $cm^3\ mol^{-1}\ s^{-1}\ cal^{-1}$ units.

| # | Reaction | $A$ | $n$ | $E_a$ | Ref. |
|---|---|---|---|---|---|
| 1 | $H + O_2 = O + OH$ | 3.55E+15 | −0.41 | 16600 | [42] |
| 13 | $HO_2 + OH = H_2O + O_2$ | 2.89E+13 | 0.00 | −497 | [49] |
| 24 | $CO + OH = CO_2 + H$ | 1.75E+05 | 1.90 | −435 | [50] |
| 25 | $CO + HO_2 = CO_2 + OH$ | 1.57E+05 | 2.18 | 17940 | [43] |
| 47 | $CH_2O + HO_2 = HCO + H_2O_2$ | 7.10E−03 | 4.50 | 6580 | [51] |
| 109 | $CH_3 + HO_2 = CH_3O + OH$ | 1.00E+12 | 0.27 | −688 | [52] |
| 110 | $CH_3 + HO_2 = CH_4 + O_2$ | 1.16E+05 | 2.23 | −3022 | [44] |
| 151 | $C_2H_6 + H = C_2H_5 + H_2$ | 1.15E+08 | 1.90 | 7530 | [46] |
| 161 | $C_2H_4 + H(+M) = C_2H_5(+M)$ | 5.40E+11 | 0.45 | 1820 | [46] |
| | Low pressure limit | 6.00E+41 | −7.62 | 6970 | |
| | $a = 0.98$, $T^{***} = 210$, $T^{*} = 984$, $T^{**} = 4374$ | | | | |
| | $H_2$ 2/$H_2O$ 6/AR 0.7/CO 1.5/$CO_2$ 2/$CH_4$ 2/$C_2H_6$ 3/HE 0.7 | | | | |
| 174 | $C_2H_5 + O_2 = C_2H_5O_2$ | 2.88E+56 | −13.82 | 14617 | [41] |
| 182 | $C_2H_5 + O_2 = C_2H_4 + HO_2$ | 7.56E+14 | −1.01 | 4749 | [41] |
| 205 | $CH_3CHO + H = CH_3CO + H_2$ | 1.11E+13 | 0.00 | 3110 | [53] |
| 206 | $CH_3CHO + O = CH_3CO + OH$ | 5.94E+12 | 0.00 | 1868 | [a] |
| 207 | $CH_3CHO + OH = CH_3CO + H_2O$ | 2.00E+06 | 1.80 | 1300 | [54] |
| 209 | $CH_3CHO + CH_3 = CH_3CO + CH_4$ | 1.76E+03 | 2.79 | 4950 | [a] |
| 210 | $CH_3CHO + HO_2 = CH_3CO + H_2O_2$ | 3.01E+12 | 0.00 | 11920 | [55] |
| 213 | $CH_3CHO + OH = CH_3 + HOCHO$ | 3.00E+15 | −1.08 | 0 | [54] |
| 214 | $CH_3CHO + OH = CH_2CHO + H_2O$ | 1.72E+05 | 2.40 | 815 | [54] |
| 247 | $C_2H_4 + O = CH_3 + HCO$ | 8.56E+06 | 1.88 | 183 | [56] |
| 248 | $C_2H_4 + O = CH_2CHO + H$ | 4.99E+06 | 1.88 | 183 | [56] |
| 249 | $C_2H_4 + OH = C_2H_3 + H_2O$ | 2.09E+06 | 2.01 | 1160 | [57] |
| 263 | $C_2H_3 + O_2 = CH_2O + HCO$ | 1.70E+29 | −5.31 | 6500 | [58] |
| 264 | $C_2H_3 + O_2 = CH_2CHO + O$ | 5.50E+14 | −0.61 | 5260 | [58] |
| 652 | $1\text{–}2C_3H_6O = C_2H_4 + CH_2O$ | 6.00E+14 | 0.00 | 60000 | [59] |
| 672 | $EP = C_2H_5COOH + C_2H_4$ | 1.60E+13 | 0.00 | 50000 | [b] |
| | Low pressure limit | 1.31E+17 | −0.99 | 11880 | |
| | $a = 0.24$, $T^{***} = 1.0$, $T^{*} = 1.00E{+}10$, $T^{**} = 6.71E{+}09$ | | | | |
| 682 | $EP + H = EP3J + H_2$ | 6.66E+05 | 2.50 | 6756 | [4][c] |
| 683 | $EP + H = EP2J + H_2$ | 2.52E+14 | 0.00 | 7300 | [4][c] |
| 684 | $EP + H = EPEJ + H_2$ | 1.20E+06 | 2.40 | 2583 | [4][c] |
| 688 | $EP + O = EPEJ + OH$ | 7.66E+05 | 2.41 | 1140 | [4][c] |
| 690 | $EP + OH = EP3J + H_2O$ | 5.28E+09 | 0.97 | 1586 | [4][c] |
| 691 | $EP + OH = EP2J + H_2O$ | 1.15E+11 | 0.51 | 63 | [4][c] |
| 692 | $EP + OH = EPEJ + H_2O$ | 1.15E+11 | 0.51 | 63 | [4][c] |
| 693 | $EP + OH = EPMJ + H_2O$ | 5.28E+09 | 0.97 | 1586 | [4][c] |
| 699 | $EP + HO_2 = EP2J + H_2O_2$ | 2.16E+12 | 0.00 | 14400 | [b] |
| 700 | $EP + HO_2 = EPEJ + H_2O_2$ | 3.61E+03 | 2.5 | 10530 | [b] |
| 760 | $C_2H_5COOH + O_2 = CH_3CHCOOH + HO_2$ | 2.00E+13 | 0.0 | 44300 | [19] |
| 761 | $C_2H_5COOH + H = CH_2CH_2COOH + H_2$ | 6.66E+05 | 2.5 | 6756 | [19] |
| 762 | $C_2H_5COOH + H = CH_3CHCOOH + H_2$ | 2.54E+14 | 0.0 | 7300 | [19] |
| 763 | $C_2H_5COOH + O = CH_2CH_2COOH + OH$ | 9.81E+05 | 2.4 | 4750 | [19] |
| 764 | $C_2H_5COOH + O = CH_3CHCOOH + OH$ | 2.20E+13 | 0.0 | 3280 | [19] |
| 765 | $C_2H_5COOH + OH = CH_2CH_2COOH + H_2O$ | 5.28E+09 | 1.0 | 1586 | [19] |
| 766 | $C_2H_5COOH + OH = CH_3CHCOOH + H_2O$ | 1.15E+11 | 0.5 | 63 | [19] |
| 770 | $C_2H_5COOH + HO_2 = CH_3CHCOOH + H_2O_2$ | 2.16E+12 | 0.0 | 14400 | [b] |

[a] Curran estimate based on fit of available data in Nist Standard Reference Database [17].
[b] Developed in this study.
[c] Analogy to methyl butanoate.

with the agreement deteriorating as conditions move from lean to rich. At $\phi = 0.3$ at 800 K, the experiments show that 11.3% of the fuel has been consumed. At these conditions, the mechanism predicts a 32.9% consumption of ethyl propanoate. Under rich conditions, Fig. 5a shows that agreement is worse, with the mechanism predicting 28.5% fuel consumption at 800 K, while the data only shows a 6.4% consumption.

This is indicative of the model's performance at rich conditions, which is considerably worse than at stoichiometric and lean. Fig. 5 shows that, not only does the model over-predict the reactivity of the fuel, it also over-predicts the consumption of ethylene and propanoic acid. Carbon dioxide and formaldehyde concentrations are well captured by the model, which also adequately describes the profiles of water, carbon monoxide and methane.

The updated model from this study was also tested against previous shock tube ignition delay data [19]. This ignition data was collected behind reflected shock waves at pressures of 1 and 4 atm and between 1100–1670 K over a range of equivalence ratios, $\phi = 0.25\text{–}1.5$.

The updated model's agreement with the previous shock tube ignition delay data is not as good as the original but it is still satisfactory, with the model predictions marginally slower than before, Figs. 6 and 7. The main discrepancy in agreement between model and experiment occurs for lean mixtures at high temperatures, for both the high and low pressure data sets. This is mainly due to the increase in the rate constant for the elimination reaction. Under lean conditions, the fuel radical species play a more important role in the overall reactivity of the system (relative to rich and stoichiometric) [19] but these species are now produced in smaller concentrations as more of the fuel is being converted to ethylene and propanoic acid.

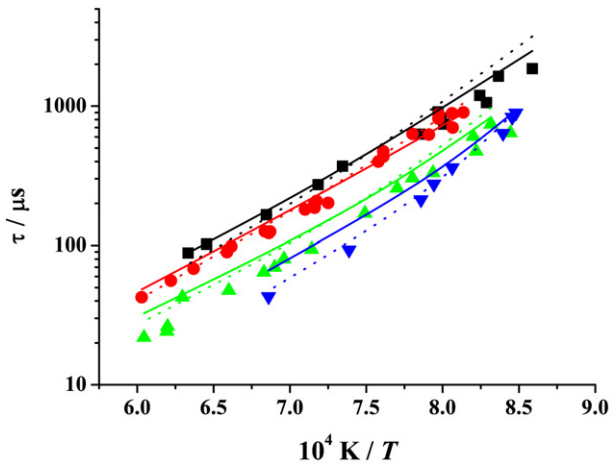


**Fig. 6.** Ignition delay times for ethyl propanoate in Ar mixtures at 1 atm, (■) $\phi = 1.5$ (1.5% fuel, 6.5% $O_2$), (●) $\phi = 1.0$ (1.0% fuel, 6.5% $O_2$), (▲) $\phi = 0.5$ (1.0% fuel, 13.0% $O_2$), (▼) $\phi = 0.25$ (1.0% fuel, 26.0% $O_2$). Symbols are experimental results. Symbols and dotted lines—Metcalfe et al. [19], solid lines—this study.

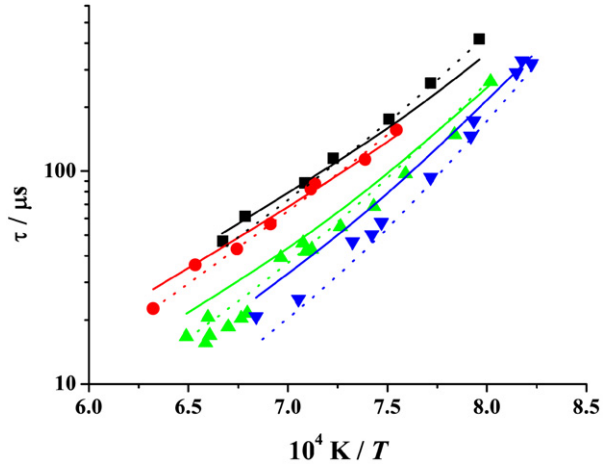


**Fig. 7.** Ignition delay times for ethyl propanoate in Ar mixtures at 4 atm, (■) $\phi = 1.5$ (1.5% fuel, 6.5% $O_2$), (●) $\phi = 1.0$ (1.0% fuel, 6.5% $O_2$), (▼) $\phi = 0.5$ (1.0% fuel, 13.0% $O_2$), (■) $\phi = 0.25$ (1.0% fuel, 26.0% $O_2$). Symbols are experimental results. Symbols and dotted lines—Metcalfe et al. [19], solid lines—this study.

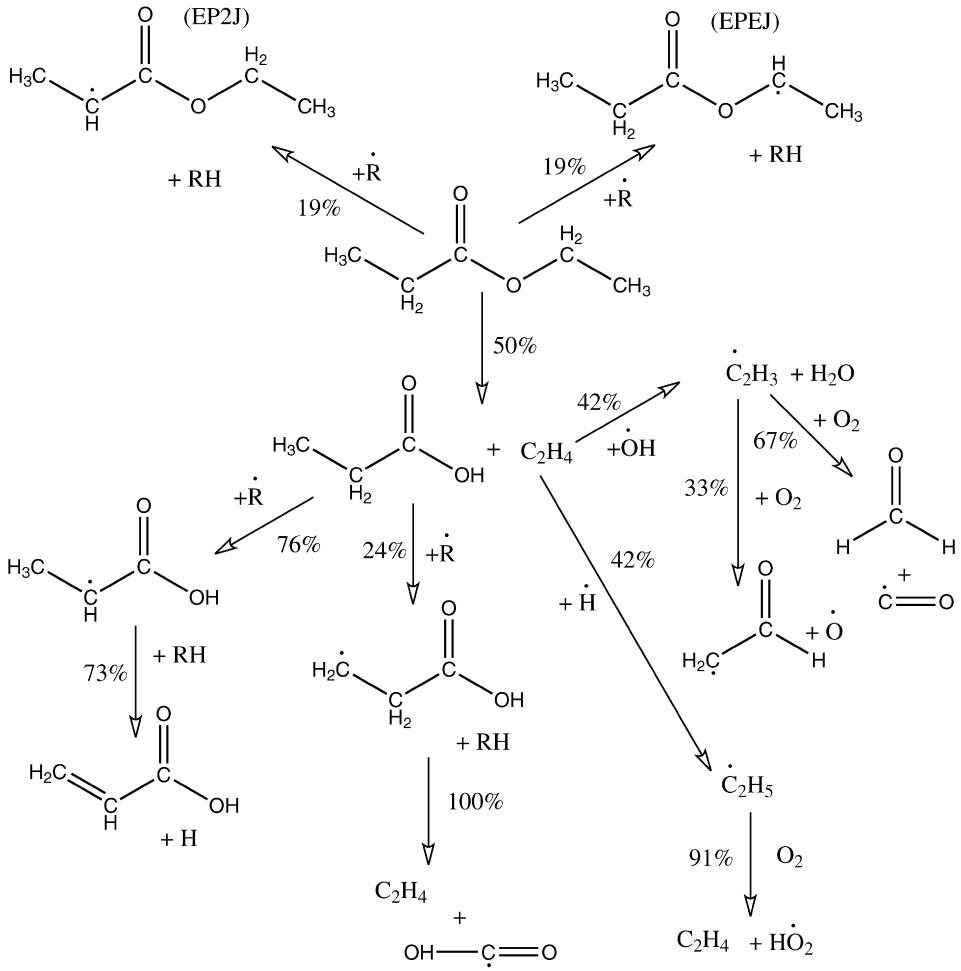


**Fig. 8.** Decomposition of ethyl propanoate at 10.0 atm, $\phi = 1.0$ and 900 K. Percentages indicate percent of parent species being converted to daughter species.

### 4.3. Rate of production analysis

In an attempt to better understand the oxidation of ethyl propanoate under jet-stirred reactor conditions, a rate of production analysis was carried out using a stoichiometric mixture of 0.1% EP, 0.65% $O_2$, at 10 atm pressure and at a temperature of 900 K. In the equation arrays below, the percentage over the arrows is the percentage of the parent species forming the daughter species. The reactions are reversible but a single headed arrow is used to show how the reaction proceeds. A synopsis of the major pathways is depicted in Fig. 8.

*4.3.1. Ethyl propanoate*

At 900 K, 94% of ethyl propanoate has been consumed. This temperature was chosen because it is in the middle of the temperature range, where the two major intermediates (ethylene and propanoic acid) are near their peak concentrations. The reactions involved in the consumption of ethyl propanoate are:

$$EP \xrightarrow{50\%} C_2H_5COOH + C_2H_4, \quad (R672)$$

$$EP + \dot{O}H \xrightarrow{12\%} EP2J + H_2O, \quad (R691)$$

$$EP + \dot{O}H \xrightarrow{12\%} EPEJ + H_2O, \quad (R692)$$

$$EP + \dot{H} \xrightarrow{7\%} EP2J + H_2, \quad (R683)$$

$$EP + \dot{H} \xrightarrow{6\%} EPEJ + H_2, \quad (R684)$$

$$EP + \dot{O}H \xrightarrow{5\%} EP3J + H_2O, \quad (R690)$$

$$EP + \dot{O}H \xrightarrow{5\%} EPMJ + H_2O, \quad (R693)$$

$$EP + \dot{O} \xrightarrow{1\%} EPEJ + \dot{O}H, \quad (R688)$$

$$EP + \dot{H} \xrightarrow{1\%} EP3J + H_2. \quad (R682)$$

Half of the fuel is consumed through the six-centered elimination reaction, with the remainder undergoing hydrogen abstraction reactions to form fuel radical species, the nomenclature of which is explained in Fig. 1. Under shock tube conditions previously studied [19], this elimination reaction proved to be much more dominant. It was found that 96% of ethyl propanoate was predicted to be consumed through this pathway at 1200 K, 1 atm pressure, and at the same stoichiometry of $\phi = 1.0$. The effect that the differing conditions has on the fate of ethyl propanoate is highlighted further when you consider that the rate constant used in the original mechanism was four times slower than the number used in this study but still had a much larger contribution to the decomposition of the fuel.

As already mentioned, almost all the fuel has been consumed at 900 K. In order to ensure that the reactivity at low concentrations was representative over the experimental range, this study was repeated at 820 K, as at this point only 51% of the ethyl propanoate has been consumed. It produced very similar results to those at 900 K, with 58% of ethyl propanoate reacting to form propanoic acid and ethylene.

*4.3.2. Fuel radical species*

At 900 K, EP2J isomerizes to EPMJ. The other important radical species, EPEJ decomposes entirely into acetaldehyde and propionyl radical. The propionyl radical has a simple reaction pathway, producing ethyl radical and carbon monoxide. Acetaldehyde undergoes several reactions with various radicals:

$$CH_3CHO + \dot{O}H \xrightarrow{30\%} \dot{C}H_3 + HOCHO, \quad (R213)$$

$$CH_3CHO + H\dot{O}_2 \xrightarrow{25\%} CH_3\dot{C}O + H_2O_2, \quad (R210)$$

$$CH_3CHO + \dot{O}H \xrightarrow{20\%} \dot{C}H_2CHO + H_2O, \quad (R214)$$

$$CH_3CHO + \dot{H} \xrightarrow{15\%} CH_3\dot{C}O + H_2, \quad (R205)$$

$$CH_3CHO + \dot{C}H_3 \xrightarrow{5\%} CH_3\dot{C}O + CH_4, \quad (R209)$$

$$CH_3CHO + \dot{O}H \xrightarrow{3\%} CH_3\dot{C}O + H_2O, \quad (R207)$$

$$CH_3CHO + \dot{O} \xrightarrow{2\%} CH_3\dot{C}O + \dot{O}H. \quad (R206)$$

*4.3.3. Propanoic acid*

Propanoic acid undergoes hydrogen abstraction primarily by hydroxyl radicals and hydrogen atoms:

$$C_2H_5COOH + \dot{O}H \xrightarrow{45\%} CH_3\dot{C}HCOOH + H_2O, \quad (R766)$$

$$C_2H_5COOH + \dot{H} \xrightarrow{24\%} CH_3\dot{C}HCOOH + H_2, \quad (R762)$$

$$C_2H_5COOH + \dot{O}H \xrightarrow{20\%} \dot{C}H_2CH_2COOH + H_2O, \quad (R765)$$

$$C_2H_5COOH + H\dot{O}_2 \xrightarrow{4\%} CH_3\dot{C}HCOOH + H_2O_2, \quad (R770)$$

$$C_2H_5COOH + \dot{H} \xrightarrow{3\%} \dot{C}H_2CH_2COOH + H_2, \quad (R761)$$

$$C_2H_5COOH + \dot{O} \xrightarrow{3\%} CH_3\dot{C}HCOOH + \dot{O}H, \quad (R764)$$

$$C_2H_5COOH + \dot{O} \xrightarrow{1\%} \dot{C}H_2CH_2COOH + \dot{O}H. \quad (R763)$$

The main intermediate of propanoic acid oxidation, $CH_3\dot{C}HCOOH$, is mostly converted to propenoic acid and a hydrogen atom via $\beta$-scission. At this temperature, propenoic acid appears to be a relatively stable molecule. It can be seen in Figs. 2a–5a (dashed lines) that propenoic acid is predicted by the mechanism but was not measured in appreciable quantities experimentally.

The prediction of propenoic acid by the mechanism is a flaw as it is not observed in the jet-stirred reactor. The model produces propenoic acid through the loss of a hydrogen atom from the secondary radical of propanoic acid, a reaction described in the reverse direction with a rate constant for $\dot{H}$ addition to propene [48]. The other pathway considered for the decomposition of $CH_3\dot{C}HCOOH$, is the formation of methyl ketene through the loss of a hydroxyl group, but this pathway does not compete at this temperature.

$CH_3\dot{C}HCOOH$ is a resonantly stabilized radical as it can also exist in the form $CH_3C{=}C\dot{O}OH$. It may be appropriate to consider the reaction of this stabilized radical with molecular oxygen to produce a low temperature chemistry consumption pathway, an option not considered when the mechanism was originally developed to describe high temperature shock tube ignition delay times. Also, it can be seen in Figs. 2–5 that the propenoic acid concentration persists until around 1000 K and then starts to be consumed. This is due to the fact that only simple decomposition reactions are included in the current mechanism, also a remnant of the original high temperature mechanism validation. At this temperature the propenoic acid decomposes through C–C bond scission to form a vinyl plus a hydro-carboxyl radical, and through C–O bond scission to produce a propenoyl and an hydroxyl radical. Addition of abstraction reactions involving propenoic acid and their subsequent pathways would improve the model's performance as the propenoic acid would be consumed more quickly resulting in lower peak concentrations.

The other intermediate of propanoic acid oxidation is $\dot{C}H_2CH_2$-COOH which decomposes to $C_2H_4$ and $HO\dot{C}{=}O$ radical. The radical in turn produces hydroxyl radical and carbon monoxide.

*4.3.4. Ethylene*

Ethylene is not only produced from propanoic acid but also in large quantities from ethyl propanoate. It too is consumed by hydrogen abstraction reactions:

$$C_2H_4 + \dot{H} + M \xrightarrow{42\%} \dot{C}_2H_5 + M, \quad (R161)$$

$$C_2H_4 + \dot{O}H \xrightarrow{42\%} \dot{C}_2H_3 + H_2O, \quad (R249)$$

$$C_2H_4 + \dot{O} \xrightarrow{7\%} \dot{C}H_3 + H\dot{C}O, \quad (R247)$$

$$C_2H_4 + CH_2O \xrightarrow{5\%} 1\text{–}2C_3H_6O, \quad (R652)$$

$$C_2H_4 + \dot{O} \xrightarrow{4\%} \dot{C}H_2CHO + \dot{H}. \quad (R248)$$

The two main products of ethylene oxidation at 900 K are ethyl and vinyl radicals. Ethyl radical almost exclusively reacts with molecular oxygen:

$$\dot{C}_2H_5 + O_2 \xrightarrow{91\%} C_2H_4 + H\dot{O}_2, \quad (R182)$$

$$\dot{C}_2H_5 + O_2 \xrightarrow{8\%} C_2H_5\dot{O}_2. \quad (R174)$$

Examining the ethylene pathways more carefully, it can be seen that nearly 40% of all ethylene produced helps cycle $\dot{H}$ into $H\dot{O}_2$.

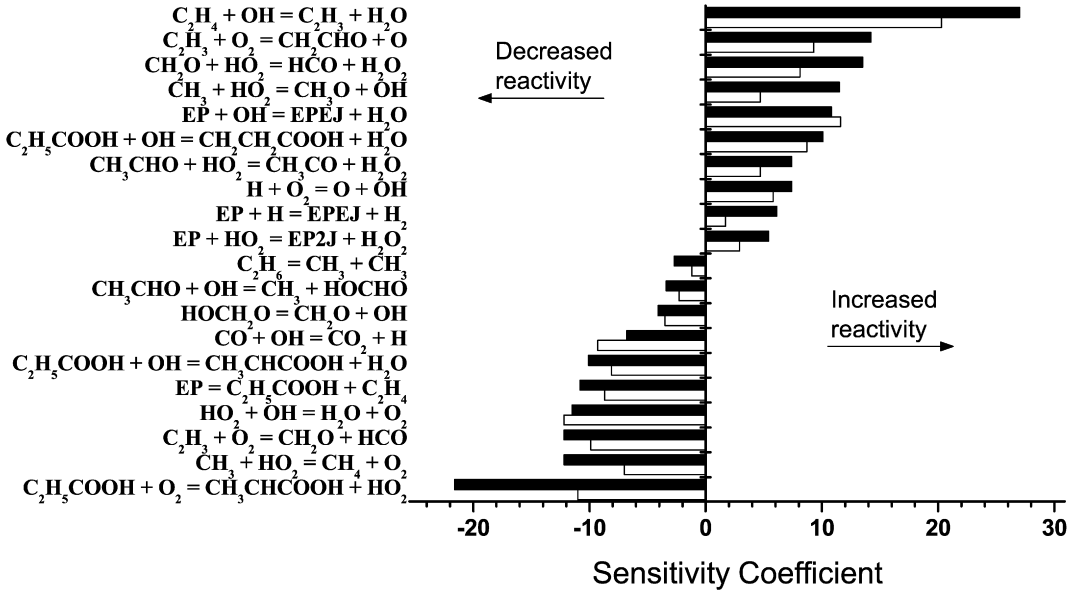


**Fig. 9.** Sensitivity coefficients for 0.1% ethyl propanoate in Argon at 900 K and 10 atm. (■) $\phi = 1.0$, (□) $\phi = 0.3$. Coefficient represents the percent change in [CO] when increasing both the forward and reverse rate coefficient of each reaction by a factor of two.

Ethylene plus $\dot{H}$ producing ethyl radical and ethyl radical plus $O_2$ reacting to form ethylene and $H\dot{O}_2$ has a net reaction of $\dot{H} + O_2 \longleftrightarrow H\dot{O}_2$.

Vinyl radical also reacts with molecular oxygen via:

$$\dot{C}_2H_3 + O_2 \xrightarrow{67\%} CH_2O + H\dot{C}O, \quad \text{(R263)}$$

$$\dot{C}_2H_3 + O_2 \xrightarrow{33\%} \dot{C}H_2CHO + \dot{O}. \quad \text{(R264)}$$

At 900 K, the propagation reaction producing formaldehyde and formyl radical is the dominant pathway but as the temperature increases the chain branching pathway becomes more important, increasing the effect that ethylene chemistry has on the overall reactivity of ethyl propanoate.

### 4.4. Sensitivity analysis

A sensitivity analysis of the updated mechanism was performed by multiplying both the forward and reverse rate constants of *all* reactions in the mechanism by a factor of two to see what effect a particular rate had on the overall reactivity of the system. Carbon monoxide concentration was used as an indicator of global reactivity. We chose carbon monoxide in our sensitivity analysis as it is generally a good indicator of reaction progress and it is sensitive not only to ethyl propanoate consumption, but also to propanoic acid and ethylene consumption which are formed very quickly from the parent fuel. Choosing ethyl propanoate concentration as a sensitivity indicator is a poor choice as the fuel very quickly becomes propanoic acid and ethylene and thus only the unimolecular decomposition reaction and some abstraction reactions from the fuel by $\dot{H}$ and $\dot{O}H$ radicals show any significant sensitivity.

The analysis was carried out at 900 K, using both lean ($\phi = 0.3$) and stoichiometric mixtures, with 0.1% fuel in each case. The results can be seen in Fig. 9. The sensitivity coefficient is defined as the percent change in carbon monoxide concentration relative to the baseline concentration. A positive coefficient indicates an increase in concentration and an overall increase in reactivity, while a negative coefficient indicates a decrease in carbon monoxide concentration and thus an overall decrease in reactivity.

Examining Fig. 9 further, the importance of ethylene chemistry is evident:

$$C_2H_4 + \dot{O}H \longleftrightarrow \dot{C}_2H_3 + H_2O. \quad \text{(R249)}$$

The above reaction is the most important one affecting carbon monoxide concentration at 900 K for both stoichiometric and lean mixtures. This reaction is the main source of vinyl radicals in the system, which as discussed previously, plays a dominant role in the overall reactivity of the system. This is reinforced by the positive sensitivity for the reaction between vinyl and molecular oxygen producing $\dot{C}H_2CHO$ and atomic oxygen. This is a chain branching reaction, therefore increasing the rate of this reaction increases the radical pool, and the global reactivity. Conversely, the other sensitive vinyl radical plus $O_2$ reaction, producing formaldehyde and a formyl radical, has a negative sensitivity. Increasing the rate of this reaction causes it to compete with the chain branching pathway, thus reducing the overall reactivity.

The third and fourth reactions of greatest importance in Fig. 9 are reactions involving the hydroperoxyl radical:

$$CH_2O + H\dot{O}_2 \longleftrightarrow H\dot{C}O + H_2O_2, \quad \text{(R47)}$$

$$CH_3 + H\dot{O}_2 \longleftrightarrow CH_3\dot{O} + \dot{O}H. \quad \text{(R109)}$$

Both of these reactions have a positive sensitivity as they produce reactive hydroxyl radicals. The former produces them indirectly, through the decomposition of hydrogen peroxide.

The reaction of hydroxyl and ethyl propanoate producing EPEJ and water also has a positive sensitivity. EPEJ is the most reactive of the fuel radical species produced at these conditions and it leads to the formation of ethyl radicals as shown in the rate of production analysis. It is more important under lean conditions as the increase in radical species leads to more EPEJ being produced through hydrogen abstraction from the fuel.

This is also evident in the system's sensitivity to hydrogen atoms. Increasing both of the reactions:

$$\dot{H} + O_2 \longleftrightarrow \dot{O} + \dot{O}H, \quad \text{(R1)}$$

$$EP + \dot{H} \longleftrightarrow EPEJ + H_2, \quad \text{(R684)}$$

increases the reactivity of the system. It would be expected that the reaction of the fuel with hydrogen atoms would compete with reaction (R1), which is the most important high-temperature chain branching reaction in combustion, and thus would have an inhibiting effect and not a promoting effect as observed. However, the generation of ethyl radicals from the EPEJ radical returns the hydrogen atoms to the system as described above and thus has the observed positive sensitivity.

The reaction between propanoic acid and hydroxyl radical is interesting as it has a positive sensitivity:

$$C_2H_5COOH + \dot{O}H \longleftrightarrow \dot{C}H_2CH_2COOH + H_2O. \quad (R765)$$

This is surprising as this reaction competes with ethylene for hydroxyl radicals, which has already been shown to be the most important promoting reaction at these conditions. This fact is offset as the primary radical produced by the abstraction of a $\dot{H}$ atom from propanoic acid by hydroxyl radical, $\dot{C}H_2CH_2COOH$, decomposes to produce ethylene and $HO\dot{C}{=}O$.

The chain branching reaction $\dot{H} + O_2 \longleftrightarrow \dot{O} + \dot{O}H$, has a positive sensitivity coefficient. This reaction between hydrogen and molecular oxygen is the most important chain branching reaction in high temperature combustion kinetics but its sensitivity diminishes at lower temperatures due to the stabilisation reaction, $\dot{H} + O_2 + M \longleftrightarrow H\dot{O}_2 + M$.

The next two reactions in Fig. 9 involve hydrogen atom abstraction from the fuel and both have positive sensitivity coefficients:

$$EP + \dot{H} \longleftrightarrow EPEJ + H_2, \quad (R684)$$

$$EP + H\dot{O}_2 \longleftrightarrow EP2J + H_2O_2. \quad (R699)$$

The reactivity of the first reaction has already been alluded to as EPEJ is a reactive species. In contrast, at 900 K, EP2J effectively does not react as it isomerizes to EPMJ. The positive sensitivity coefficient associated with this reaction is due to the hydrogen peroxide that is also produced, which leads to the formation of hydroxyl radicals.

Fig. 9 also highlights the reactions that inhibit the reactivity of the system. There are several that have a negative sensitivity as they compete with ethylene for hydroxyl radicals:

$$CH_3CHO + \dot{O}H \longleftrightarrow \dot{C}H_3 + HOCHO, \quad (R213)$$

$$CO + \dot{O}H \longleftrightarrow CO_2 + \dot{H}, \quad (R24)$$

$$C_2H_5COOH + \dot{O}H \longleftrightarrow CH_3\dot{C}HCOOH + H_2O, \quad (R766)$$

$$H\dot{O}_2 + \dot{O}H \longleftrightarrow H_2O + O_2. \quad (R13)$$

The reaction between propanoic acid and hydroxyl radical not only consumes a reactive radical but also produces two unreactive species. Despite producing a $\dot{H}$ atom in its decomposition, $CH_3\dot{C}HCOOH$ also produces propenoic acid, which lies dormant at this temperature. The most suppressive reaction involving a hydroxyl radical occurs with the hydroperoxyl radical. Here, two reactive species are converted into two stable species.

At first glance, a negative sensitivity for the decomposition of ethane to two reactive methyl radicals (R151) is counter-intuitive. When examined further, this reaction actually proceeds almost exclusively in the reverse direction so it is a chain terminating step, consuming two methyl ($\dot{C}H_3$) radicals. This reaction competes with the reaction of methyl radicals with hydroperoxyl radicals (R109), producing two reactive radicals:

$$\dot{C}H_3 + \dot{C}H_3 + M \longleftrightarrow C_2H_6 + M, \quad (R151)$$

$$\dot{C}H_3 + H\dot{O}_2 \longleftrightarrow CH_3\dot{O} + \dot{O}H. \quad (R109)$$

Another surprising result is the negative effect of increasing the six-centered elimination reaction forming propanoic acid and ethylene from ethyl propanoate. This was also seen in the shock tube sensitivity analysis but only at high temperatures (1600 K). This result may be highlighting a flaw in the method used for the jet-stirred reactor sensitivity analysis. Carbon monoxide concentration was used as an indicator for global reactivity, however a major source of carbon monoxide comes from an intermediate produced from a fuel radical species. Thus, increasing the elimination reaction decreases the amount of fuel radical species produced, resulting in a lower concentration of carbon monoxide. Fuel consumption however, is increased by approximately 1.5%, so this result may not be a true reflection of the sensitivity of this reaction.

The final reaction included in Fig. 9 has the largest negative sensitivity coefficient.

$$C_2H_5COOH + O_2 \longleftrightarrow CH_3\dot{C}HCOOH + HO_2. \quad (R760)$$

Increasing the rate of this reaction inhibits reactivity for two reasons. Firstly, it consumes oxygen which is very important in the vinyl radical chemistry, and secondly it causes less propanoic acid to form the reactive primary radical, $\dot{C}H_2CH_2COOH$, instead increasing the concentration of the secondary radical, which produces unreactive propenoic acid.

## 5. Conclusions

Ethyl propanoate oxidation was studied in a jet-stirred reactor at 10 atm, with a residence time of 0.7 s, over a range of stoichiometries ($\phi = 0.3$–$2.0$). This data was used to validate a previously published detailed kinetic mechanism describing ethyl propanoate oxidation. This was a good test of the model as it had previously only been tested against ignition delay times, a measure of global reactivity. The species profiles measured in the reactor allow the evolution of the chemistry to be simulated. The mechanism performed quite well, except in the case of the propanoic acid profile which it under-predicted by a factor of three. Changes were made to improve agreement with this data, the most significant being a factor of four increase in the rate of the six-centered elimination reaction. The results are shown in Figs. 2–5, with the updated mechanism performing very well.

The rate of production analysis reveals that the elimination reaction plays a much smaller role in the decomposition of ethyl propanoate relative to hydrogen abstraction reactions under the jet-stirred reactor conditions compared to the shock tube conditions previously studied.

The sensitivity analysis reinforced the results from the shock tube study, once again highlighting the importance of ethylene chemistry and also vinyl plus molecular oxygen reactions. Hydroxyl radicals were also found to be much more important at these lower temperatures.

A problem with the modeling study is the prediction of relatively large concentrations of propenoic acid, a compound measured in only trace amounts experimentally. Further work is warranted to develop a better understanding of the chemistry of propanoic and propenoic acid oxidation.

## Acknowledgment

Wayne Metcalfe thanks the Environmental Protection Agency of Ireland for a Doctoral Fellowship (2004-PHD4-8-M1).

## Supplementary material

Supplementary material for this article may be found on ScienceDirect, in the online version.

Please visit DOI: 10.1016/j.combustflame.2008.09.007.

## References

[1] B. Metz, O.R. Davidson, P.R. Bosch, R. Dave, L.A. Meyer, Climate Change 2007: Mitigation. Contribution of Working Group III to the Fourth Assessment Report of the Intergovernmental Panel on Climate Change, IPCC/Cambridge Univ. Press, Cambridge, UK/New York, 2007.
[2] J.M. Simmie, Prog. Energy Combust. Sci. 29 (2003) 599–634.
[3] P. Dagaut, S. Gaïl, M. Sahasrabudhe, Proc. Combust. Inst. 31 (2007) 2955–2961.
[4] E.M. Fisher, W.J. Pitz, H.J. Curran, C.K. Westbrook, Proc. Combust. Inst. 28 (2000) 1579–1586.
[5] B.I. Parsons, C.J. Danby, J. Chem. Soc. (1956) 1795–1798.

[6] B.I. Parsons, C. Hinshelwood, J. Chem. Soc. (1956) 1799–1803.
[7] B.I. Parsons, J. Chem. Soc. (1956) 1804–1809.
[8] D.E. Hoare, T.M. Li, A.D. Walsh, Proc. Combust. Inst. 11 (1967) 879–887.
[9] A.J. Marchese, M. Angioletti, F.L. Dryer, in: International Symposium on Combustion (2004), Work-in-progress poster 1F1–03.
[10] S. Gaïl, M.J. Thomson, S.M. Sarathy, S.A. Syed, P. Dagaut, P. Diévart, A.J. Marchese, F.L. Dryer, Proc. Combust. Inst. 31 (2007) 305–311.
[11] S.M. Sarathy, S. Gail, S.A. Syed, M.J. Thomson, P. Dagaut, Proc. Combust. Inst. 31 (2007) 1015–1022.
[12] W.R. Schwartz, C.S. McEnally, L.D. Pfefferle, J. Phys. Chem. 110 (2006) 6643–6648.
[13] S. Dooley, H.J. Curran, J.M. Simmie, Combust. Flame 153 (2008) 2–32.
[14] A.T. Blades, P.W. Gilderson, Can. J. Chem. 38 (1960) 1412–1415.
[15] H.E. O'Neal, S.W. Benson, J. Phys. Chem. 71 (1967) 2903–2921.
[16] A.T. Blades, H.S. Sandhu, Int. J. Chem. Kinet. 3 (1971) 187–193.
[17] J.A. Barnard, A.T. Cocks, T.K. Parrott, J. Chem. Soc. Faraday Trans. 72 (1976) 1456–1463.
[18] A. El-Nahas, J.W. Bozzelli, J.M. Simmie, H.J. Curran, W. Metcalfe, S. Dooley, J. Phys. Chem. A 111 (2007) 3727–3739.
[19] W.K. Metcalfe, S. Dooley, H.J. Curran, J.M. Simmie, A.M. El-Nahas, M.V. Navarro, J. Phys. Chem. A 111 (2007) 4001–4014.
[20] P. Dagaut, M. Cathonnet, J.-P. Rouan, R. Foulatier, A. Quilgars, J.-C. Boettner, F. Gaillard, H. James, J. Phys. E Instrum. 19 (1986) 207–209.
[21] P. Dagaut, F. Lecomte, S. Chevailler, M. Cathonnet, Combust. Sci. Technol. 148 (1999) 27–57.
[22] P. Dagaut, J. Luche, M. Cathonnet, Combust. Sci. Technol. 165 (2001) 61–84.
[23] P. Dagaut, A. Nicolle, Combust. Flame 140 (2005) 161–171.
[24] P. Dagaut, O. Mathieu, A. Nicolle, G. Dayma, Combust. Sci. Technol. 177 (2005) 1767–1791.
[25] P. Dagaut, A. Nicolle, Int. J. Chem. Kinet. 37 (2005) 406–413.
[26] C.M. Lund, L. Chase, HCT—A general computer program for calculating time-dependent phenomena involving one-dimensional hydrodynamics, transport, and detailed chemical kinetics, Lawrence Livermore National Laboratory report UCRL-52504, revised (1995).
[27] S.W. Benson, Thermochemical Kinetics, Wiley, New York, 1976.
[28] E.R. Ritter, J.W. Bozzelli, Int. J. Chem. Kinet. 23 (1991) 767–778.
[29] T. Lay, J.W. Bozzelli, A.M. Dean, E.R. Ritter, J. Phys. Chem. 99 (39) (1995) 14514–14527.
[30] E.W. Kaiser, T.J. Wallington, M.D. Hurley, J. Platz, H.J. Curran, W.J. Pitz, C.K. Westbrook, J. Phys. Chem. A 104 (35) (2000) 8194–8206.
[31] S.L. Fischer, F.L. Dryer, H.J. Curran, Int. J. Chem. Kinet. 32 (2000) 713–740.
[32] H.J. Curran, S.L. Fischer, F.L. Dryer, Int. J. Chem. Kinet. 32 (2000) 741–759.
[33] X.L. Zheng, T.F. Lu, C.K. Law, C.K. Westbrook, H.J. Curran, Proc. Combust. Inst. 30 (2005) 1101–1109.
[34] C.K. Westbrook, M.M. Thornton, W.J. Pitz, P.C. Malte, Proc. Combust. Inst. 22 (1988) 863–871.
[35] P. Dagaut, J.-C. Boettner, M. Cathonnet, Int. J. Chem. Kinet. 22 (1990) 641–664.
[36] C.J. Brown, G.O. Thomas, Combust. Flame 117 (1999) 861–870.
[37] H.J. Curran, P. Gaffuri, W.J. Pitz, C.K. Westbrook, Combust. Flame 114 (1998) 149–177.
[38] H.J. Curran, P. Gaffuri, W.J. Pitz, C.K. Westbrook, Combust. Flame 129 (2002) 253–280.
[39] K.R. Doolan, J.C. Mackie, C.R. Reid, Int. J. Chem. Kinet. 18 (1986) 575–596.
[40] E.L. Petersen, D.M. Kalitan, S. Simmons, G. Bourque, H.J. Curran, J.M. Simmie, Proc. Combust. Inst. 31 (2007) 447–454.
[41] J.D. DeSain, S.J. Klippenstein, J.A. Miller, C.A. Taatjes, J. Phys. Chem. A 107 (2003) 4415–4427.
[42] J.P. Hessler, J. Phys. Chem. A 102 (1998) 4517–4526.
[43] X. You, H. Wang, E. Goos, C.-J. Sung, S.J. Klippenstein, J. Phys. Chem. A 111 (2007) 4031–4042.
[44] N.K. Srinivasan, J.V. Michael, L.B. Harding, S.J. Klippenstein, Combust. Flame 149 (2007) 104–111.
[45] A.W. Jasper, S.J. Klippenstein, L.B. Harding, Proc. Combust. Inst. 32 (2009), doi: 10.1016/j/proci.2008.05.036.
[46] G.P. Smith, D.M. Golden, M. Frenklach, N.W. Moriarty, B. Eiteneer, M. Goldenberg, C.T. Bowman, R.K. Hanson, S. Song, W.C. Gardiner Jr., V.V. Lissianski, Z. Qin, GRI-Mech 3.0. http://www.me.berkeley.edu/gri_mech/.
[47] http://c3.nuigalway.ie/.
[48] H.J. Curran, Int. J. Chem. Kinet. 38 (2006) 250–275.
[49] M.A. Mueller, R.A. Yetter, F.L. Dryer, Proc. Combust. Inst. 27 (1998) 177–184.
[50] S.G. Davis, A.V. Joshi, H. Wang, F. Egolfopoulos, Proc. Combust. Inst. 30 (2005) 1283–1292.
[51] S.H. Robertson, P.W. Seakins, M.J. Pilling, Chapter 2: Elementary reactions, in: M.J. Pilling (Ed.), Low-Temperature Combustion and Autoignition, in: Comprehensive Chemical Kinetics, vol. 35, Elsevier, Amsterdam, 1997, pp. 125–234, ISBN: 9780444824851.
[52] N.K. Srinivasan, J.V. Michael, L.B. Harding, S.J. Klippenstein, Combust. Flame 149 (2007) 104–111.
[53] D.A. Whytock, J.V. Michael, W.A. Payne, L.J. Stief, J. Chem. Phys. 65 (1976) 4871–4875.
[54] P.H. Taylor, M.S. Rahman, M. Arif, B. Dellinger, P. Marshall, Proc. Combust. Inst. 26 (1996) 497–504.
[55] D.L. Baulch, C.J. Cobos, R.A. Cox, C. Esser, P. Frank, T. Just, J.A. Kerr, M.J. Pilling, J. Troe, R.W. Walker, J. Warnatz, J. Phys. Chem. Ref. Data 21 (1992) 411–429.
[56] D.L. Baulch, C.T. Bowman, C.J. Cobos, R.A. Cox, T. Just, J.A. Kerr, M.J. Pilling, D. Stocker, J. Troe, W. Tsang, R.W. Walker, J. Warnatz, J. Phys. Chem. Ref. Data 34 (3) (2005) 757–1397.
[57] A. Liu, W.A. Mulac, C.D. Jonah, J. Phys. Chem. 92 (1988) 3828–3833.
[58] N.M. Marinov, Int. J. Chem. Kinet. 31 (1999) 183–220.
[59] M.C. Flowers, J. Chem. Soc. Faraday Trans. 73 (1977) 1927–1935.